Waste Management 154 (2022) 232–244

Contents lists available at ScienceDirect

Waste Management

journal homepage: www.elsevier.com/locate/wasman

Effect of polymer type on the properties of polypropylene composites with high loads of spent coffee grounds

Mariana Marques, Luis F.F.F. Gonçalves *, Carla I. Martins, Mário Vale, Fernando M. Duarte

IPC—Institute of Polymer and Composites, University of Minho, 4804-533 Guimarães, Portugal

ARTICLE INFO

Keywords:
Spent Coffee Ground (SCG)
Polymer-matrix composites
Polypropylene
Mechanical properties
Waste reuse

ABSTRACT

The main focus of this work is to study the processability and characteristics of highly loaded spent coffee grounds (SCG) thermoplastic polymer composites, for sustainable applications. SCG powder was characterized in terms of size distribution, moisture, morphology and thermal stability. Polymer/SCG composites were prepared by extrusion compounding. Polypropylene (PP) homopolymer and copolymer were used as the polymeric matrix. Upon compounding by extrusion composites were injection moulded and characterized for its physical, morphological and mechanical properties in order to determine the effect of polymer type and filler content. Morphological characteristics of the composites were investigated using optical microscopy and SEM analysis. The results for PP homopolymer showed little deterioration of the mechanical properties when using the highest SCG load. In the case of PP homopolymer, the greatest variations occurred when increasing from 0 to 20 %. With higher SCG loads, the measured properties changed little. PP copolymer showed a more continuous pattern of properties decay with increasing SCG load, especially for tensile strength, elongation at break and impact strength. Regarding PP copolymer, with maximum SCG load, the tensile strength decreased from 26.8 GPa (neat PP) to 10.8 GPa, the elongation at break showed a drop of more than 95 %, while the Young's modulus increased from 800 MPa to 1160 MPa. This research work has shown that SCG can be used as fillers in the preparation of environmentally friendly composites with SCG load up to 60 wt% thus contributing to the reuse of waste generated by the coffee industry.

1. Introduction

Nowadays, there is a growing demand for new materials based on natural ones. The current trend, due to greater environmental awareness, is to look for more sustainable materials or simply to reuse those that are considered waste, but could be used so that their useful life is extended and added value is achieved. One such material is Spent Coffee Grounds (SCG). Coffee is one of the most popular beverages all over the world, meaning that several million tons of SCG are produced every year (McNutt & He, 2019). SCG are a waste material that results from the treatment of roasted coffee powder with hot water in order to obtain instant coffee. It has been estimated that for each kg of soluble coffee 2 kg of wet SCG are generated (Mata et al., 2018). SCG are normally discarded as waste and thrown into landfills or burned in order to achieve their disposal. Both processes raise important environmental issues, therefore the need to find methods or processes for valorisation of SCG residues. SCG are made up mainly of cellulose, lignin and hemicellulose and recently there has been an increasing interest in reusing this waste in areas such as extraction of useful natural organic compounds (Ballesteros et al., 2014), organic composting (Ronga et al., 2016), energy recovery (Kang et al., 2017), thermal insulation improvement in construction materials (Lachheb et al., 2019), the production of active carbon (Jung et al., 2016), ethanol (Mussatto et al., 2012) and biodiesel (Goh et al., 2020)(Atabani et al., 2019). Polymer composites are also another option (Essabir et al., 2018).

Plastics have found increasingly more applications in our daily lives, ranging from packaging and containers to parts of appliances or automobiles. With increasing environmental concerns, undoubtedly in large part related to the consumption of non-renewable petroleum-based products, there has been a focus in the development of new environmentally friendly composite materials. The use of natural materials such as fibres in polymer reinforcement has been considered, as there is often the need to add additives/fillers or reinforcements to plastics in order to improve or change certain properties. Besides meeting environmental concerns, natural fibres present other advantages over the synthetic ones namely, low density, natural abundance, biodegradability, low cost,

* Corresponding author.
E-mail address: luisf@dep.uminho.pt (L.F.F.F. Gonçalves).

https://doi.org/10.1016/j.wasman.2022.10.009
Received 7 March 2022; Received in revised form 29 August 2022; Accepted 9 October 2022

high toughness, high stiffness, low energy recovery, no health hazard, and CO_2 neutral after burning (Pickering et al., 2016)(Väisänen et al., 2016)(Gurunathan et al., 2015)(Sanjay et al., 2019). Examples of increasingly used natural fibres that have been added to plastics include wood flour, cork, jute, bamboo, rice hull, kenaf, among other examples (Martins et al., 2022)(Martins & Gil, 2020)(Murayama et al., 2019)(Borges et al., 2018)(Väisänen et al., 2017). Therefore, natural fibres are increasingly considered as a feasible substitute to the traditional reinforcing materials for the manufacturing of composites. SCG can be regarded as particles composed mainly by natural fibres. Up to now, SCG were used in the preparation of polymeric composites with loads up to 20 wt% (García-García et al., 2015)(Essabir et al., 2018). In order to meet increasingly demanding environmental concerns, so crucial nowadays, it is necessary to reuse waste materials and incorporate them in new materials that include a higher percentage of feedstock from sustainable sources.

The main goal of this work is to investigate the characteristics of the SCG and its suitability for the production of high loaded SCG polymer-based composites, so that they can further be transformed into products by polymer processing techniques such as injection moulding or extrusion techniques. The main idea is to increase the amount of this disposable natural resource up to 60 wt% in the composite in order to diminish the use of non-renewable resources. The polymeric matrix, at this load percentage, would be regarded as a binder. Due to degradation of lignocellulosic materials at high temperatures, the processing temperatures allowed to prepare the composites are limited to about 200 °C, which means that the SCG, as any other natural compound, can only be used with commodity thermoplastics such as polyethylene (PE) or polypropylene (PP). Two different types of polypropylene matrices, homopolymer and copolymer, were evaluated. PP random copolymer features ethylene units incorporated randomly in the polypropylene chain, while PP homopolymer contains only propylene monomer. This difference in the polymeric chain conveys different properties to the two types of PP, and so, it is expected that this may also influence the polymer's ability to disperse the SCG particles within it. Another goal of our study is therefore to assess the ability of each type of polymer to disperse the SCG particles, and to assess the extent to which the SCG particles affect the properties of each of the PP types. The composites were prepared using loads of SCG between 20 and 60 wt% by twin screw extrusion followed by injection moulding to prepare samples for mechanical testing and the physical, morphological and mechanical properties were measured. In addition, thermogravimetry analysis (TGA) was used to study the thermal stability of the SCG at the temperatures commonly used to process PP.

2. Materials and methods

2.1. Materials

Two commercial polypropylene grades, a propylene-ethylene random copolymer ISPLEN PR 230 C1E and a polypropylene homopolymer ISPLEN PP 040 C1E, both supplied by REPSOL, with a melt flow index of 1.6 g/10 min (at 230 ℃) and 3.0 g/10 min (at 230 ℃) respectively, were used as the matrix. The Spent coffee grounds (SCG) were collected from local coffee shops in the form of a wet cake after extraction with hot water for the beverage preparation. The SCG were initially dried at room temperature for about one week with manually stirring to prevent fungal breeding. Subsequently, they were dried in an oven at 80 °C for about 12 h and stored in closed containers.

2.2. SCG characterization

2.2.1. Granulometric analysis

The granulometric analysis was performed using the RETSCH AS200 BASIC equipment with six sieves with mesh dimensions of 1000, 500, 300, 212, 150 and 106 μm. Five samples of 150 g each were used for the characterization of the materials granulometry. Samples were sieved for 5 min at a vibrate amplitude of 2.6 mm.

2.2.2. Humidity analysis

Two types of moisture content analysis were performed in order to characterize the SCG: the moisture content after the beverage preparation and the moisture content of the dried SCG. The moisture content after the beverage preparation was determined following the procedure described in DIN EN 15013. The technique consisted in drying and weighing the samples successively until a stable weight was reached. The SCG samples were first dried in an oven during 30 min, then cooled in an excitatory until room temperature was reached and then weighted using an analytical balance. This procedure was repeated continuously until the difference between two consecutive weightings was less than 1 %. Ten samples of SCG with approximately 50 g were used and an average value was calculated. The moisture content of the dried SCG was determined using a KERN MLB_N volatile meter, following the standard EN 61326–1: 2006. The measurement was performed for three different samples of SCG with approximately 5 g, at a temperature that allowed the water release (120 ℃). The moisture content, h, in percentage, is given by Eq. (1), where m_1 corresponds to the mass of the specimen with moisture and m_2 is the mass of the specimen without moisture.

$$\%h = \frac{m_1 - m_2}{m_1} \times 100 \quad (1)$$

2.2.3. Thermogravimetric analysis (TGA)

Thermogravimetric analysis (TGA Q500 from TA Instruments) was performed in order to evaluate the SCG degradation with temperature as well as to evaluate its stability during the preparation of the polymer composites by extrusion. Samples with approximately 7 mg of SCG were placed in standard alumina crucibles and subjected to a heating program from 30 °C to 600 °C at a heating rate of 10 °C/min under air atmosphere, in order to simulate the environmental degradation. To evaluate the stability of SCG and simulate the residence time inside the extruder or the injection-moulding machine, the samples were heated from 30 °C to the desired temperature at a heating rate of 10 °C/min under air atmosphere and kept at constant temperature for 30 min. This time corresponds to 3–4 times the typical residence time of the SCG inside the extruder. The temperatures tested were 140 °C, 160 °C, 180 °C, 200 °C, 220 °C and 240 °C.

2.2.4. Scanning electron microscopy (SEM)

SEM analysis of SCG samples was performed on a scanning electron microscope NanoSEM - FEI Nova 200 (FEG/SEM). The samples were fixed on stainless steel supports and coated with gold using a metallizer at 1100–1200 V, 5 mA, for 10 min.

2.3. PP/SCG composites preparation

The PP/SCG composites were prepared in a laboratory modular Leistritz LSM 30.34 intermeshing co-rotating twin-screw extruder. The extruder screw contains a series of transport elements separated by two mixing zones in order to produce the required intensive mixing together with the development of local pressure gradients. Two gravimetric feeders were used to ensure the correct loading percentages of polymer and SCG. The composite materials were prepared with different loads of SCG (20 wt%, 40 wt% and 60 wt%). PP without SCG was also prepared as reference material. Before processing, the SCG were dried in an oven at 80 °C for 4 h. The screw speed was set at 150 rpm and the temperature profile ranged from 120 °C, near the hoper, to 180 °C in the extruder die. The extruded filaments were cooled by air at room temperature and then pelletized in a mill.

PP/SCG granules were dried (4 h at 80 °C in an oven) and used to produce tensile (190 mm length × 10 mm width × 4 mm thickness) and impact specimens (130 mm length × 12 mm width × 6 mm thickness) by

injection moulding. An ENGEL VICTORY 80 injection moulding machine was used. The processing temperatures ranged from 140 °C near the hoper to 185 °C in the nozzle. The mould temperature was set at 30 °C and a cycle time of 37 s was used. An injection pressure of 2 bar, a dosing volume of 40.60 cm^3, and a cooling time of 20 s were used. All the remaining processing parameters were adjusted in order to obtain defect-free specimens.

2.4. PP/SCG composites characterization

2.4.1. Melt flow index

The melt flow index of all prepared materials was measured using DAVENTEST equipment according to ISO 1130. A load of 2.16 kg at 230 °C was used. Three measurements were made for each sample.

2.4.2. Density

The density tests were carried out by following the guidelines of Test Method B from the ASTM D792, using a solution of alcohol and water. Samples weighing about 10 g and cut from injection moulded specimens were used as specimens.

2.4.3. Optical microscopy

The PP/SCG composites were imaged by optical microscopy using a BH2 Olympus transmission microscope. Samples were cut using a microtome and placed on a glass coverslip with Canada Balm. The images were obtained using a Leica MTV-3 digital camera and analysed by a Leica Application Suite software.

2.4.4. Scanning electron microscopy (SEM)

SEM analysis of PP/SCG composites was performed on a scanning electron microscope NanoSEM - FEI Nova 200 (FEG/SEM). The samples were fixed on stainless steel supports and coated with gold using a metallizer at 1100–1200 V, 5 mA, for 10 min. The images were obtained on fractured composites surfaces from specimens after Izod Impact tests.

2.4.5. Mechanical properties

Tensile properties were obtained at room temperature according to ASTM D638 and using the universal test machine Instron 5969 equipped with an SVE 2 Non-Contacting Video Extensometer. The cross-head speed was fixed at 5 mm/min using a 50 kN load cell. For each material, ten different specimens were subjected to tensile tests and average values of tensile strength, Young's modulus and elongation at break were calculated.

Flexural properties were obtained at room temperature using a universal test machine INSTRON 5969. For each material, ten specimens were subjected to a flexural test according to ISO 178 at a test speed of 2 mm/min and average values of flexural modulus and strength were calculated.

Izod impact tests were conducted in a CEAST 6545/000 machine according to the procedure described by methodology A of ASTM D256. The specimens were notched in a MITUTOYO NO.250–351 equipment. For each material, ten specimens were subjected to impact test and average values of absorbed energy were calculated.

3. Results and discussion

3.1. SCG characterization

3.1.1. Granulometric characterization

The granulometric analysis provides information about the size distribution of the SCG particles. As shown in Fig. S1 (support information), an average of 75 % of the volume fraction of the SCG sample had particles with sizes equal or lower than 300 μm. A similar outcome was obtained by Sousa and Ferreira (Massaro Sousa & Ferreira, 2019), which found that, using sieves of size aperture ranging from 150 μm to 2400 μm, the mass fraction of SCG particles retained in sieves of size aperture above 600 μm was only 20 % of the total. The higher mass fraction found by these authors was about 30 % for particle size of around 310 μm. It should be emphasized that the particle size as well as the particle size distribution is dependent of the previous coffee grain milling process. Therefore, different results can be obtained from SCG collected from other waste points.

3.1.2. Humidity analysis

Numerous research studies pointed out the resistance to water as one of the most important factors in the fabrication of natural fibre composites. Moisture has great influence in the composite fabrication process as water presence can cause dimensional changes and deterioration of properties (Almudaihesh et al., 2020). SCG is a residue with a fine particle size, high moisture and high organic load, that is obtained as residue after coffee preparation using raw coffee powder and boiling water (McNutt & He, 2019). The high absorption of water in materials containing natural fibres, such as SCG, is due to the presence of hydroxyl groups at the surface of those natural fibres that have high-affinity towards water molecules (García-García et al., 2015)(Gurunathan et al., 2015). Fig. S2 (support information) shows the evolution of the total mass loss during the SCG drying process in the oven. The samples present major changes in mass loss within the first two hours. After 3 h, the total amount of moisture loss was about 30 wt%. Approximately after 5 h of drying, the samples reached a plateau of approximately 50 wt% of total mass loss. This amount did not change substantially after 5 h indicating that the samples were already dried at that time. However, it should be emphasized once more that these results are valid for the SCG derived from the preparation of the expresso coffee beverage that originates SCG in the form of cake. Although other types of beverage preparation can lead to different amounts of moisture in the SCG, the results show that SCG can retain a great amount of water (around 100 % of its weight). Therefore, SCG composites must be protected from highly moisture environment for lasting applications. On the other hand, this highly sensibility to moisture could be advantageous for biodegradable applications.

3.1.3. Thermogravimetric analysis – TGA

Fig. 1 presents the TGA results for SCG, showing the variation of weight of the SCG with temperature. The dashed line represents the weight loss while the bold line represents the derivative weight loss. The plot shows four distinct regions of weight variation, as previous reported by García-García et al. (García-García et al., 2015): i) the first, with a weight loss of about 4 wt%, occurs between the initial temperature and about 110/120 °C, and corresponds to the loss of residual moisture of the SCG (Ballesteros et al., 2015)(Baek et al., 2013); ii) the second region, ranging from 200 °C and 325 °C corresponds to the depolymerization of hemicellulose, with a sharp weight loss, corresponding to about 50 wt% of the total weight loss, and with a peak of weight loss at 300 °C. Similar results were also obtained by Bejenari and Lisa (Bejenari & Lisa, 2019) for temperatures above 230 °C and were attributed to thermal depolymerization of hemicelluloses. García-García et al. reported a weight loss of 43 % for this stage but within a temperature range between 170 °C – 350 °C; iii) the third region, ranging between 325 °C and 430 °C, corresponds to cellulose degradation, with a weight loss of about 20 wt%. In several studies, in regions 2 and 3, ranging approximately between 200 °C and 500 °C, a steep slope is observed in the TGA curves, corresponding to a significant decrease in weight due to the release of volatile hydrocarbons resulting from the rapid thermal decomposition of cellulose, hemicellulose and lignin. Cellulose and hemicellulose decompose in the temperature range of 150 °C to 390 °C, while lignin has a wider range of decomposition temperature, which can range between 250 °C and 500 °C (Tangmankongworakoon, 2019) (Chen & Kuo, 2010)(Sanchez-Silva et al., 2012); iv) Finally, at temperatures higher than 430 °C, the fourth and last region presents a weight loss of about 22 wt% due to decomposition of remaining lignin. The remaining mass is formed by the mineral material transformed into

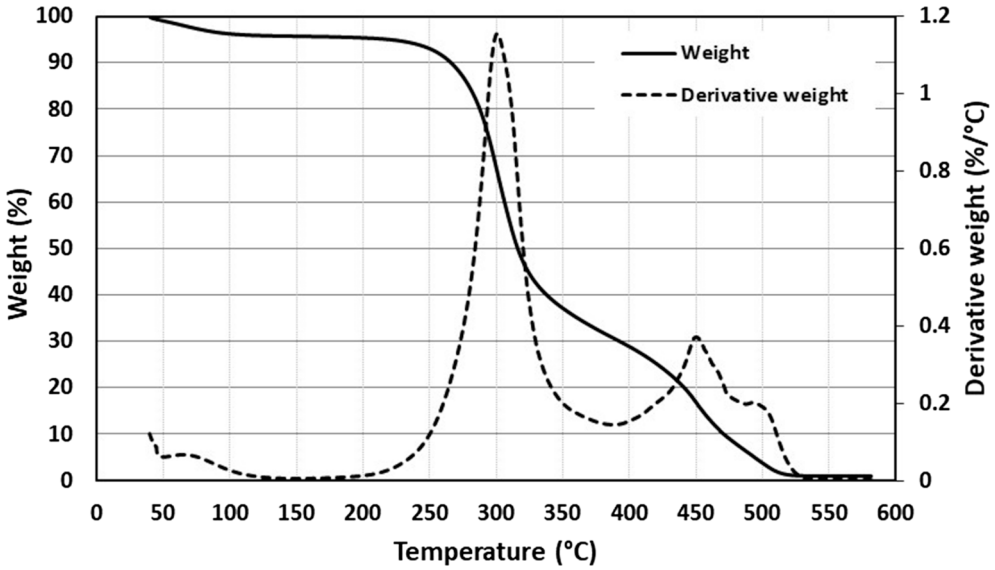

Fig. 1. Thermogravimetric (TGA) and derivative TGA curves of SCG.

ashes (metallic oxides) (Chen & Kuo, 2010)(Sefain & El-Kalyoubi, 1984). Similar behaviours are reported in scientific studies related to lignocellulosic biomass (Zarrinbakhsh et al., 2016).

Fig. S3 (support information) shows the complete isothermal weight loss curves (including heating period up to the test temperature followed by 30 min at constant temperature) for SCG. In the first 8 min of heating (which corresponds to a maximum heating of 120 °C) the weight loss that occurs in all samples (about 4 wt%) corresponds to the evaporation of water. From that moment on, there is a certain stability in the weight loss up to about 20 min of heating.

The insert of Fig. S3 (support information) shows the section of the isothermal weight loss curves of the SCG corresponding to the first 25 min of heating at constant temperature. For the various isometric curves, it is observed that up to the curve corresponding to 180 °C, the weight loss is less than 5 wt%. For temperatures 240 °C and 260 °C, the weight loss after 30 min is about 10 wt% and 17 wt%, respectively. Up to a temperature of 180 °C there is a tendency for a greater weight loss with increasing test temperature. The curves show similar behaviour in the first 8 min of the test. The curve obtained at 200 °C shows a greater weight loss in relation to the other curves at about 5 min after the beginning of the test, which increases with time, although it follows the trend of the other curves up to 200 °C. Using temperatures equal or higher than 220° C, there is a more pronounced weight loss after 16 min, following a different trend compared to the isothermals obtained with temperatures lower than 200 °C. This situation indicates a process of thermal degradation of the SCG (decomposition of the hemicellulose and cellulose as mentioned above).

These results show that the loss of performance of the composite materials due to the degradation of the fillers is residual when using processing temperatures up to 180 °C. Processing is still possible at around 200 °C as long as the residence time of the material in the extruder does not exceed 8/10 min. It should also be noted that although the weight loss is relatively small up to the isotherm of 180 °C, the relatively low weight loss observed in the first 10 min, which corresponds to less than 3 wt%, could mean the loss of volatile organic compounds, that might originate composites with voids. To this value of weight loss, it is also necessary to add the weight loss occurring in the initial minutes of heating coming from the moisture present in the fillers. Therefore, as long as the processing temperature does not exceed 200 °C, the mechanical performance of the composites may not be compromised by the degradation of the SCG fillers, but may be influenced by the presence of voids resulting from the release of volatiles.

3.1.4. Scanning electron microscopy (S.E.M.)

Fig. S4 (support information) shows SEM images of the SCG obtained with different magnifications. The images show that the granules have an irregular and porous surface that might allow a good interaction with the polymeric matrix. The porous surface also explains the high absorption/adsorption capacity of the SCG towards moisture. The analysed sample, also shows a typical size distribution of particles resulting from the milling process, consisting of very small particles, with dimensions less than 100 μm, and particles with dimensions in the order of 500 μm.

3.2. PP/SCG composites characterization

3.2.1. Melt flow index

Melt flow index (MFI) measurements were used as simple method to examine the flow characteristics of PP/SCG composites in the molten state. Fig. 2 presents the MFI results of neat PP and PP/SCG composites. Both PP used have different MFI. An increase of the MFI is observed after the inclusion of the SCG filler. However, the increase of MFI is more pronounced when PP homopolymer is used. The amount of SCG seems to have a negligible effect on melt flow index, with only the composites with 60 wt% of SCG showing a subtle increase of MFI compared to the other PP/SCG composites. The increase in MFI might be due to some oils present in the SCG that could have a lubricating effect (Ballesteros et al., 2014). These MFI results are quite the opposite from other MFI results reported for other fiber/polymer composites. Gallegher et al. (Gallagher & McDonald, 2013) reported a decrease of MFI of wood plastic composites with increasing amounts of wood fiber. Similar results were reported by Tasdemir et al. (Tasdemır et al., 2009) for PP/wood fiber composites. In our case, it is generally found that even with the addition of high loads of SCG the processability of the composites is not negatively affected but instead it is improved. This can be confirmed by the fact that composites with high loads of SCG were successfully processed by extrusion and injection molding.

3.2.2. Density

The dimensional stability of the composites can be influenced by its density. Low-density composites can absorb moisture and retain more water than high-density composites since low-density composites present more voids, porosities, and open spaces (Taib & Julkapli, 2018). Natural fibres have densities in the range of 1.2 – 1.6 $g.cm^{-3}$ (Karimah et al., 2021) while neat PP has a density of 0.9 $g.cm^{-3}$. By the rule of mixture this would mean that adding SCG to neat PP would lead to an

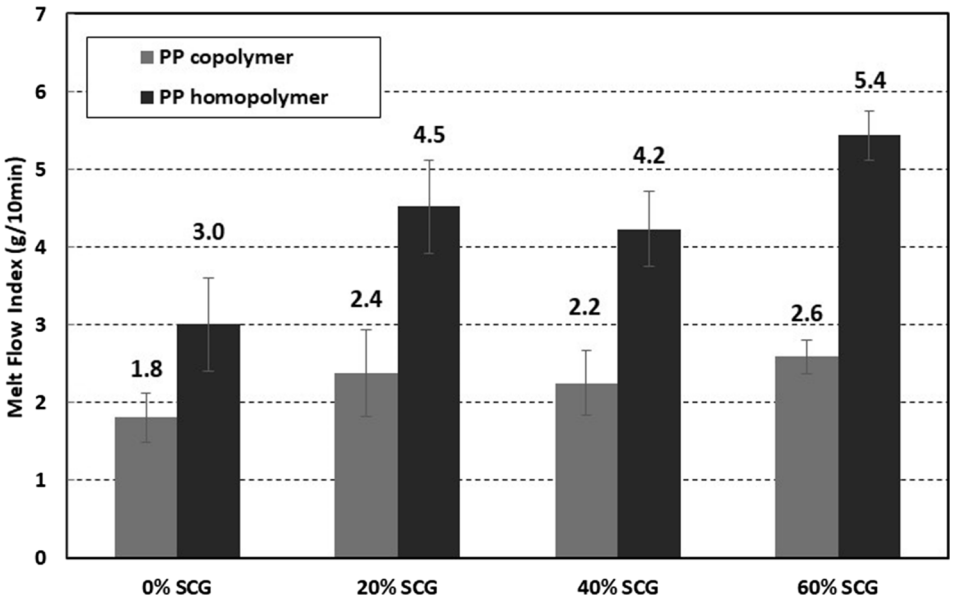

Fig. 2. MFI of neat PP and of PP/SCG composites with different amounts of SCG filler.

increase in the density of the composite. Fig. 3 shows the results obtained for the density of neat PP and of PP/SCG composites. The incorporation of SCG in the PP matrices leads to an increase in density compared to neat PP. Equally, increasing the SCG load leads to a slight increase in the PP/SCG composite density. Similar results were reported for composites reinforced with natural fibres (Soleimani et al., 2008) (Rosa et al., 2009)(Shinoj et al., 2010). This behaviour is normally attributed to the higher density of the natural fibre (Soleimani et al., 2008). Rosa et al. (Rosa et al., 2009) observed only a expressionless increase in the composite density and attributed it to the lack of penetration of the PP matrix within the natural fibres thus producing composites with lower densities than the expected.

3.2.3. *Optical microscopy*

Optical microscopy makes it possible to assess the degree of dispersion and distribution of particles within the polymer matrix. Fig. 4 shows the images obtained by optical microscopy of composites for both PP copolymer and PP homopolymer. The images show SCG particles with different sizes and geometries heterogeneously distributed within the PP matrix. The distributive mixing is equivalent in both samples, as the SCG particles are equally scattered throughout the entire sample. The micrographs also show the presence of some larger particles mixed with a great number of smaller particles. For both PP homopolymer and PP copolymer composites with 20 wt% of SCG there are no visible signs of agglomeration of SCG particles. With 60 wt% SCG load, the micrographs also show the presence of particles of different sizes equally distributed throughout the entire sample indicating that the amount of SCG had no visible effect on the distributive mixing of the SCG within the PP matrix, although the higher load of SCG promotes greater discontinuity of the matrix. The larger difference in SCG particle size is due to the process of coffee grinding as observed previously by the granulometric analysis to the SCG. Another possibility is the mechanism of erosion of the SCG particles during extrusion that yields smaller fibres that are then distributed in the matrix (looking like small dots). This is also corroborated by the presence of smaller SCG particles when 60 wt% SCG is used. Therefore, the amount of SCG load has no visible effect on the distributive mixing of the SCG within the PP matrix, but has some influence on the disruption of the SCG particles and on its dispersion. Note that the white spaces observed in the images of Fig. 4 (marked by the red arrows) result both from scratches produced on the sample during the

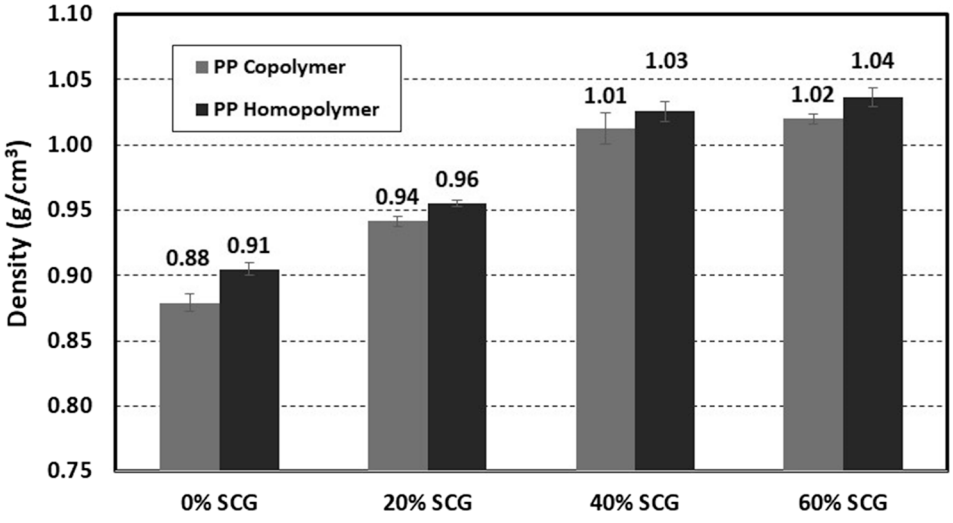

Fig. 3. Density of neat PP and of PP/SCG composites with different amounts of SCG filler.

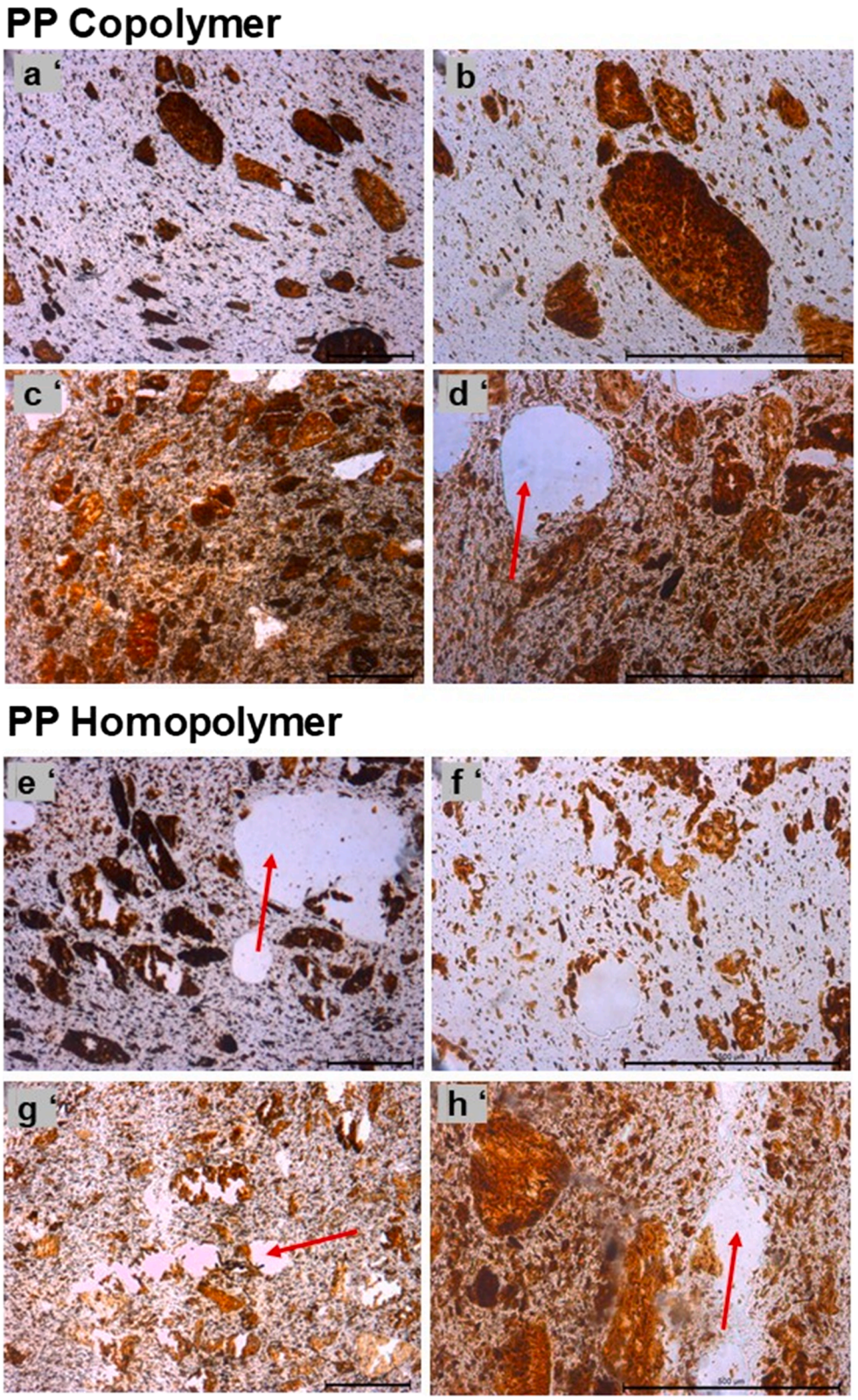

Fig. 4. (a-d) - Morphology images of PP copolymer/SCG composites: a) 20 wt% obtained with 4x magnification; (b) 20 wt% and 10x magnification; c) 60 wt% obtained with 4x magnification; d) 60 wt% and 10x magnification. (e-h) - Morphology images of PP homopolymer/SCG composites: e) 20 wt% obtained with 4x magnification; (f) 20 wt% and 10x magnification; g) 60 wt% obtained with 4x magnification; h) 60 wt% and 10x magnification.

preparation for optical microscope observation and from regions where coffee grains might have been eliminated during cutting of samples.

3.2.4. Scanning electronic microscopy

Scanning electron microscopy was used to investigate the SCG surface and their interfacial adhesion with polymeric matrix. The effect of polymer type is evaluated by comparing the SEM images of the composites prepared with each PP polymer type.

Fig. 5 shows SEM images of the fractured surfaces from impact tests of PP/SCG composites obtained with different magnifications. In both cases, the images show a random filler dispersion within the polymer matrix without significant particle agglomeration, as already suggested by optical microscopy. The addition of SCG fillers to the polymer promotes the formation of discontinuities in the PP matrix. In addition, in both cases the composites show a gap zone (interfacial void) between the SCG particles and the contiguous PP matrix suggesting poor interfacial adhesion between the SCG particles and PP matrix (images 5e and 5f at 5000X magnification). Similar observations were previously

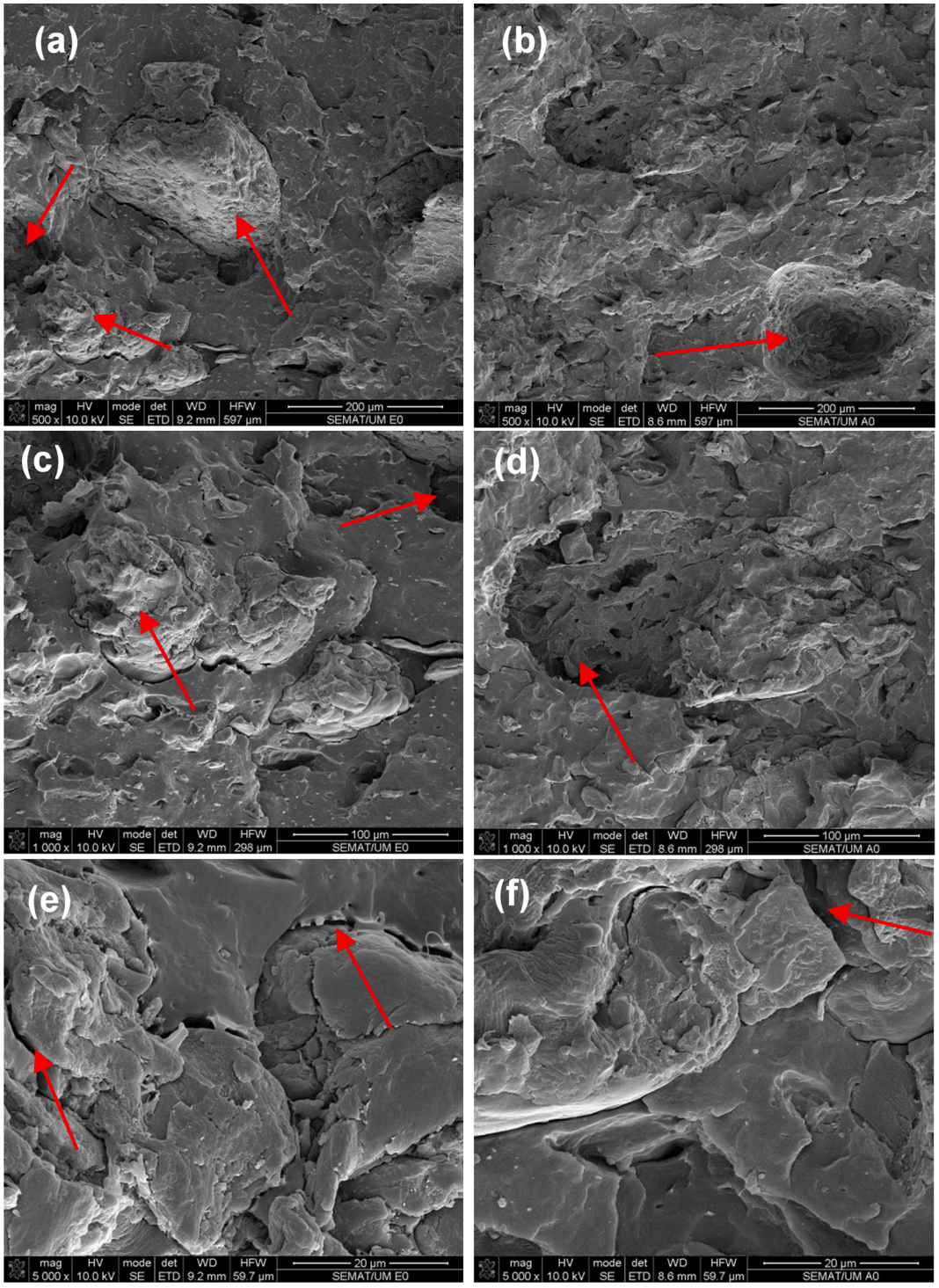

Fig. 5. SEM micrographs of PP/SCG composites (20 wt% of SCG) prepared with PP homopolymer (left, a, c, e) and PP copolymer (b, d, f) at three magnifications: 500X (a, b), 1000x (c, d) and 5000X (e, f).

reported for untreated SCG fillers within PP matrix (García-García et al., 2015). The gap zone is slightly more perceptible when using PP homopolymer (images 5c, 5e). Another indication of poor interaction between the polymer and the SCG fillers is the out-of-plane rupture surfaces between the matrix and the SCG particles. Images at 500X (5a, 5b) and 1000X (5c, 5d) magnification shows slight craters and the presence of some protuberances due to the pull-out of SCG fillers from the matrix. It would be expected, in the case of a strong interaction between polymer

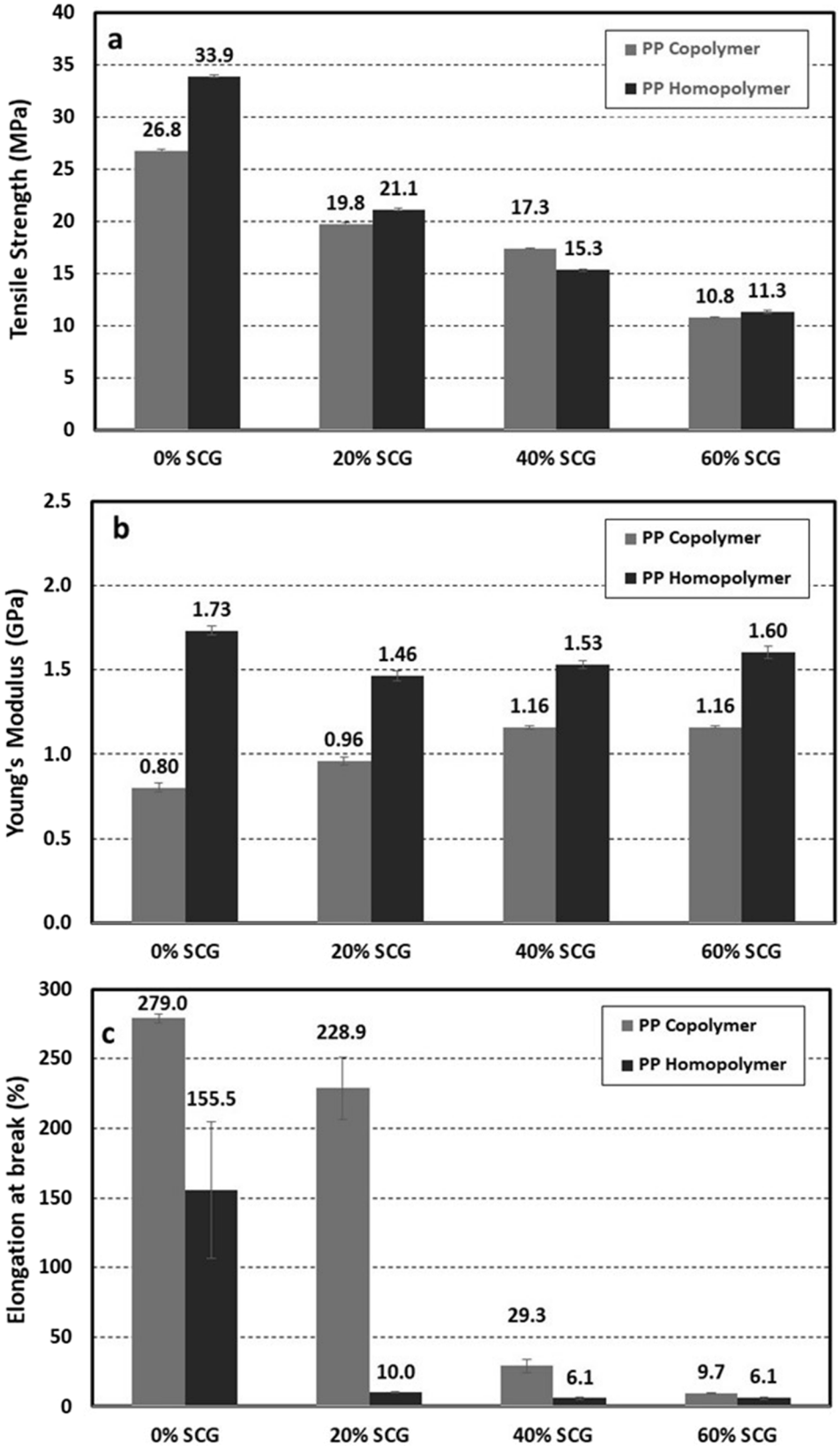

Fig. 6. Plot comparison of mechanical properties of PP/SCG composites. (a) Tensile strength, (b) Young's modulus and (c) Elongation at break.

and matrix, an in-plane fracture between filler and matrix without substantial pull-out of fillers. PP homopolymer composites (images 5a and 5c) show higher craters and protuberances due to pull-out of SCG compared to PP copolymer, which suggests lower interaction between SCG particles and PP homopolymer compared to PP copolymer. Abhilash et al. (Abhilash et al., 2021) observed, using SEM images, improved adhesion between PP copolymer and bamboo fibres compared to PP homopolymer. They reported that fractured surface of 30 % reinforced PP homopolymer showed fibre–matrix debonding and fibre pull-out as the most prominent micromechanical deformations compared to fractured surface of 30 % reinforced PP copolymer matrix, which showed fibre fracture and matrix yielding as the major factors causing deformation in addition to fibre pull-out (Abhilash et al., 2021). In the presence of good stress transfer between matrix and fibre there is less debonding and filler pull-out during impact. During deformation, debonding is the predominant process when there is poor adhesion between filler and matrix, while matrix yielding and/or filler fracture is the predominant process when adhesion is improved (Renner et al., 2010). In addition, the SEM images show the presence of micro voids, which is another indication of poor interfacial bonding between SCG particles and the PP matrix.

3.2.5. Mechanical properties

The effect of SCG on the tensile properties of the PP/SCG composites is presented in Fig. 6, where tensile strength, Young's modulus and elongation at break are shown for the composites with SCG ranging between 0 wt% and 60 wt%.

The plot in Fig. 6a show an almost linear decrease of the tensile strength with increasing amounts of SCG in both PP homopolymer and PP copolymer composites, although the decrease in this property is more pronounced for PP homopolymer. This decrease in the tensile strength can be attributed to poor adhesion between the SCG natural fibres and the PP matrix, as observed in SEM images (Fig. 5), that results in a deficient particle–matrix interface. The gap between filler and matrix hampers the proper load transfer between the PP matrix and the stiffer SCG filler, explaining the decrease of tensile strength. Similar outcomes were previously observed and reported in other published studies (Essabir et al., 2018) (Srubar et al., 2012). In addition, Baek et al. attributed the decrease in the tensile strength to the weak bond between the hydrophilic SCG filler and the hydrophobic PP matrix (Baek et al., 2013). The micro voids observed in the SEM images, originated by poor interfacial bonding between filler and matrix, hamper proper stress propagation amongst the filler and the matrix resulting in lower tensile strength (Yang et al., 2006). The high loads of SCG used in the composites makes it more difficult the wetting of the particles by the matrix, as observed in the optical microscopy images (Fig. 4c, 4d and 4h). Reis et al. attributed similar decrease in tensile strength to improper particle wetting (Reis et al., 2015).

Fig. 6b also shows a lower Young's modulus for PP copolymer composites compared to PP homopolymer composites, possibly due to the differences in the Young's modulus of the neat matrix, as neat PP homopolymer has higher modulus than PP copolymer. An increase in the Young's modulus with increasing amounts of SCG is observed for PP copolymer composites indicating an increase in its stiffness, which is accompanied by the abrupt decrease in the elongation at break, especially for composites with loads of SCG of 40 wt% and higher (see Fig. 6c). In the case of PP homopolymer, the addition of SCG to the polymer caused only a slight decrease in the Young's modulus compared to neat PP, however its effect in the elongation at break is very sever even for 20 wt% SCG. The elongation at break decreased for all composites compared to the respective neat polymer (Fig. 6c). In the case of PP homopolymer composites, the addition of SCG with any concentration lead to a remarkable decrease in the elongation at break suggesting an increase in the brittleness of the material. For the PP copolymer, with 20 wt% the elongation at break dropped from 279 to 228.9 but with increasing amounts of SCG filler the elongation at break dropped sharply as in the case of PP copolymer. This behaviour, the increase in Young's modulus and decrease of tensile strength and elongation at break with increasing SCG loading, is typical of many polymer/natural fibre systems of which there are a number of reports in the literature (Tasdemır et al., 2009). Optical microscopy images (Fig. 4) show the presence of some larger particles, which promote large discontinuities in the matrix. The presence of such large SCG particles in the polymer composite during stretching may disturb chain orientation due to the considerable larger size of fillers, compared to the orientation scale of polymeric chains, originating stress concentration locations that worsens the elongation at break and tensile strength of the composite (Zanjani et al., 2020). The drastic decrease in elongation at break can also be attributed to a high restriction in the chain movement within the polymer matrix due to the presence of high loads of fillers in the system, which eventually causes stiffness in the composite (Al-Saleh et al., 2019). This phenomenon is enlarged with the increase of the filler load within the polymer matrix. In addition, the decrease in the elongation at break might be related to agglomeration of filler at high loads or the presence of large particles, as shown by the optical microscopy images (Fig. 4), that introduce large discontinuities in the matrix, both acting as locations of stress concentration, resulting in fissure growth under the applied tensile stress. The presence of voids and other imperfections at the filler/polymer interface showed in the SEM images (Fig. 5) can also induce fracture in highly crystalline polymers as pointed out by others (Reis et al., 2015)(Srubar et al., 2012). The higher reduction in elongation at break for the PP homopolymer, compared to PP copolymer, might be due to the intrinsic inelasticity of relatively rigid PP homopolymer, as compared to PP copolymer, resulting in ineffective stress transfer between polymer matrix and SCG filler and subsequent brittle fracture (Joshi et al., 2017). The possible formation of voids and/or micro-voids, as a result of the release of volatiles that occur during processing, as observed by SEM images (Fig. 5) as well as the fracture of SCG particles due to lack of cohesion, may be two other factors that explain the pronounced degradation of the tensile strength strain and of the elongation at break observed in the PP/SCG composites.

In addition to tensile properties, three other mechanical properties were measured for the neat PP matrices and their corresponding composites: the flexural modulus, that measures the tendency of the composite material to bend, flexural strength, that measures the ability of the material to resist deformation under load and the impact strength, that measures the resistance of materials against fracture. Fig. 7a shows the flexural modulus obtained for PP/SCG composites.

The plot shows that the flexural modulus increases with increasing filler loading. Flexural strength (Fig. 7b) suffered a slight decrease for both polymers with addition of SCG, which is expected for composites with low interfacial adhesion between filler and matrix, due to stress concentration phenomena. García-García et al. attributed this decrease to the irregular size and shape of SCG particles that do not enable particle alignment during mixing (García-García et al., 2015). The irregular size and shape of SCG particles can be attested by the already discussed SEM images of the SCG particles (support information, Fig. S4). Regarding the impact strength (Fig. 7c), composites prepared with PP homopolymer exhibited relatively lower impact strength as compared to those of PP copolymer. This is mainly due to inherent properties of both PP homopolymer and PP copolymer, as neat copolymer PP showed higher impact strength compared to neat PP homopolymer. The higher impact strength of PP copolymer results from the higher inherent flexibility of polymer chains due to polyethylene groups. The decrease of impact strength with increased filler loading was previously reported (Rahman et al., 2009)(Rana et al., 2003) and is attributed to the incorporation of a more rigid natural fibre into the soft PP matrix. Natural fibres have higher modulus compared to PP, and so it is expected an increase in stress to obtain the same deformation with increasing amounts of fibre. In addition, Fig. 7c shows that the impact strength decreases with increasing SCG load. The decrease of impact strength may also be explained by high SCG loads, some SCG agglomeration and

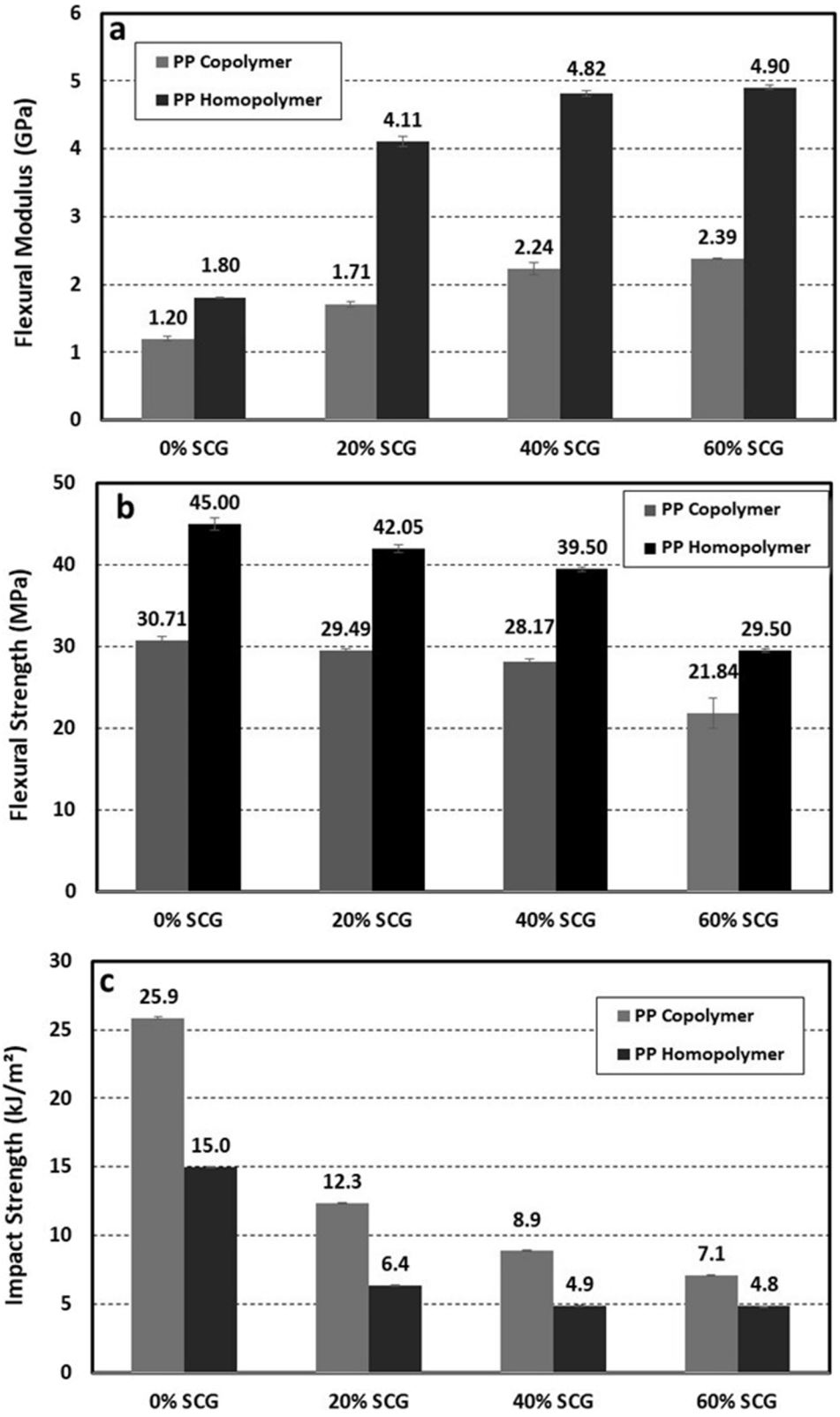

Fig. 7. (a) Flexural modulus of PP/SCG composites, (b) Flexural strength of PP/SCG composites and (c) Izod impact strength of PP/SCG composites.

by the poor interfacial interaction between SCG particles and PP matrix, as shown by optical microscopy and SEM images. Similar outcome was reported by Thomason et al. (Thomason & Rudeiros-Fernández, 2018). Poor interfacial interaction between PP and SCG enables the formation and propagation of micro-cracks at the fibre-polymer interface sections during impact conditions (García-García et al., 2015). The lower impact strength of PP homopolymer/SCG composites compared to PP copolymer/SCG composites may be explained by lower interaction between SCG particles and PP homopolymer, compared to PP copolymer, as attested by the presence of higher craters and protuberances due to pull-

out of SCG particles (SEM images in Fig. 5a and 5c) in this composite compared to PP copolymer composites. PP type (homopolymer or copolymer) showed the most significant effect on the Young's modulus of the composites. Kim et al. (Kim et al., 2014) also reported the tensile and flexural moduli of short wool fibre/PP composites as the properties that were most influenced by PP type. They suggested that variation of the wool/PP composite moduli is largely influenced by melt flow rate of the PP during the extrusion. Sallih et al. (Sallih et al., 2014) reported that PP MFI significantly affected the mechanical properties of kenaf/PP composites, with higher PP MFI generating composites with better mechanical properties compared to a lower PP MFI. This is also observed in our study, where PP homopolymer is the one having higher MFI and therefore, better mechanical properties in terms of tensile and flexural behaviour. This may be explained by better particle wetting by the PP homopolymer compared to PP copolymer. PP copolymer benefits from its molecular structure and therefore the impact strength is better in this case. The mechanical properties are strongly correlated with the degree of dispersion and distribution of the particles within the matrix, as mechanical performance is strongly conditioned by discontinuities in the matrix caused by the inclusion of fillers. The structural properties of polymer composites depend greatly on interfacial adhesion between matrix and particles, but also on concentration, particle size, morphology and spatial distribution of particle clusters (Khan et al., 2020). Best mechanical performance is normally achieved with smaller size particles (Khan et al., 2020). Large particles and the presence of particle clusters can act as defect sites, prompting the formation of cracks and inducing fracture.

Fig. 8 shows the effect of SCG on the MFI and mechanical properties. The data is normalized for comparison.

According to Fig. 8, PP homopolymer composites show the largest variation in MFI and mechanical properties when SCG increase from 0 wt% to 20 wt%. No significant changes are observed with further increases of SCG loading, with the exception of both the tensile strength and the flexural strength, which continuously decrease with increasing SCG loading. With loads higher than 20 wt%, flexural modulus increases further with increasing amounts of filler, but these increases are less pronounced compared to the first increase from 0 wt% to 20 wt% of SCG. For the other remaining properties, there are no sudden changes in properties with the increase in SCG load from 20 wt% to 60 wt%. In the case of PP copolymer composites, the variations in mechanical properties with increasing amount of SCG load are larger compared to the same properties observed in PP homopolymer composites. In this case, in addition to the tensile strength that decreases continuously with increasing amounts of SCG, the elongation at break decreases sharply by increasing the amount of SCG from 20 wt% to 40 wt%, and the impact strength decays continuously with increasing SCG load. The remaining properties do not show great changes by increasing load of SCG from 20 wt% to 40 wt% and further to 60 wt%.

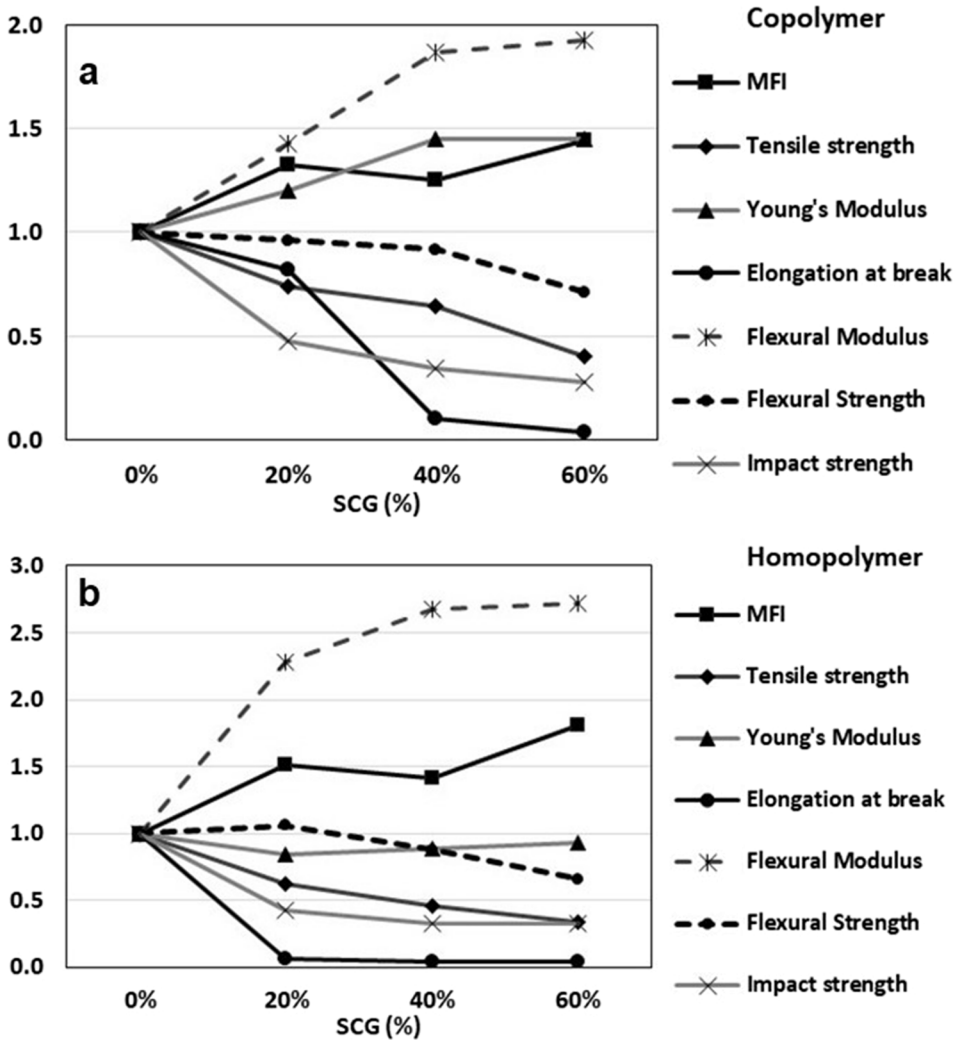

Fig. 8. Variation in the properties of the composites with the amount of SCG load (a) PP copolymer and (b) PP homopolymer. The data were normalized, with the value of 1.0 corresponding to the neat polymer.

4. Conclusions

This study has examined the production of new polymer composite materials based on SCG. Both PP copolymer and PP homopolymer with SCG percentages up to 60 wt% were produced and characterized in terms of its physical, morphological and mechanical properties.

The incorporation of SCG in the PP matrices leads to an increase in density compared to neat PP. The density increased further with increased amounts of SCG. An increase of the MFI is observed in the composites after the inclusion of the SCG. However, the increase of MFI is more pronounced when PP homopolymer is used. The greatest variations in the majority of the mechanical properties of PP homopolymer occur when increasing SCG load from 0 wt% to 20 wt%. Further increase of SCG loading up to 60 wt%, did not change considerably the mechanical performance, except for the tensile strength and flexural strength, which continuously decrease with increasing SCG loading. PP copolymer showed a continuous decay pattern of the properties, especially for tensile strength, elongation at break and impact strength. The tensile strength decreased with increasing amount of SCG load. This decrease in the tensile strength was due to poor adhesion and weak bond between the hydrophilic SCG particles and the hydrophobic PP matrix. The sharp decrease in elongation at break was due to the presence of filler at high loads that promoted larges discontinuities in the matrix. The Young's modulus has shown a slight increase in the case of PP copolymer. Impact strength also decreased with increasing amounts of SCG filler due to poor interfacial interaction between SCG particles and PP matrix and particle agglomeration. Flexural modulus showed an increase with increasing amounts of SCG filler that was most evident in the case of PP homopolymer, due to the incorporation of more rigid natural fibre into the soft PP matrix. Increasing the SCG also lead to a slight increase in PP/SCG composite densities. Optical microscopy showed distributive mixing regardless of filler concentration and the presence of SCG particles of different sizes and shapes within the polymer composite. SEM micrographs showed some gap voids surrounding the SCG filler within the PP matrix possibly explaining the lower tensile and impact strength of the PP/SCG composites compared to the neat PP. PP homopolymer composites showed higher number of craters and protuberances due to filler pull-out compared to PP copolymer, which may indicate better stress transfer from matrix to filler when using PP copolymer. In overall, PP copolymer composites showed lower Young's modulus and flexural modulus but performed better in terms of impact strength compared to PP homopolymer composites.

This research work has shown that spent coffee grounds can be used as fillers in the preparation of environmentally friendly composites with SCG load up to 60 wt% thus contributing to the reuse of waste generated by the coffee industry.

Declaration of Competing Interest

The authors declare that they have no known competing financial interests or personal relationships that could have appeared to influence the work reported in this paper.

Data availability

No data was used for the research described in the article.

Acknowledgements

This research was supported by FEDER funds through the COMPETE 2020 Programme and National Funds through FCT (Portuguese Foundation for Science and Technology) under the projects UID-B/05256/2020, UID-P/05256/2020.

Appendix A. Supplementary material

Supplementary data to this article can be found online at https://doi.org/10.1016/j.wasman.2022.10.009.

References

Abhilash, R.M., Venkatesh, G.S., Chauhan, S.S., 2021. Development of bamboo polymer composites with improved impact resistance. Polym. Polym. Compos. 29 (9_suppl), S464–S474.

Almudaihesh, F., Holford, K., Pullin, R., Eaton, M., 2020. The influence of water absorption on unidirectional and 2D woven CFRP composites and their mechanical performance. Compos. B Eng. 182, 107626.

Al-Saleh, M.A., Yussuf, A.A., Al-Enezi, S., Kazemi, R., Wahit, M.U., Al-Shammari, T., Al-Banna, A., 2019. Polypropylene/Graphene Nanocomposites: Effects of GNP Loading and Compatibilizers on the Mechanical and Thermal Properties. Materials 12 (23), 3924. https://doi.org/10.3390/ma12233924.

Atabani, A.E., Al-Muhtaseb, A.H., Kumar, G., Saratale, G.D., Aslam, M., Khan, H.A., Said, Z., Mahmoud, E., 2019. Valorization of spent coffee grounds into biofuels and value-added products: Pathway towards integrated bio-refinery. Fuel 254 (February), 115640. https://doi.org/10.1016/j.fuel.2019.115640.

Baek, B.S., Park, J.W., Lee, B.H., Kim, H.J., 2013. Development and Application of Green Composites: Using Coffee Ground and Bamboo Flour. J. Polym. Environ. 21 (3), 702–709. https://doi.org/10.1007/s10924-013-0581-3.

Ballesteros, L.F., Teixeira, J.A., Mussatto, S.I., 2014. Chemical, Functional, and Structural Properties of Spent Coffee Grounds and Coffee Silverskin. Food Bioprocess Technol. 7 (12), 3493–3503. https://doi.org/10.1007/s11947-014-1349-z.

Ballesteros, L.F., Cerqueira, M.A., Teixeira, J.A., Mussatto, S.I., 2015. Characterization of polysaccharides extracted from spent coffee grounds by alkali pretreatment. Carbohydr. Polym. 127, 347–354. https://doi.org/10.1016/j.carbpol.2015.03.047.

Bejenari, V., Lisa, G., 2019. Thermal behaviour of different types of commercial coffee and resulting coffee grounds in inert atmosphere. The influence of composition (arabica and robusta). Cellul. Chem. Technol. 53 (9), 861–868. https://doi.org/10.35812/CelluloseChemTechnol.2019.53.83. https://doi.org/10.35812/CelluloseChemTechnol.2019.53.83.

Borges, J.K., Pacheco, F., Tutikian, B., de Oliveira, M.F., 2018. An experimental study on the use of waste aggregate for acoustic attenuation: EVA and rice husk composites for impact noise reduction. Constr. Build. Mater. 161, 501–508. https://doi.org/10.1016/j.conbuildmat.2017.11.078.

Chen, W.H., Kuo, P.C., 2010. A study on torrefaction of various biomass materials and its impact on lignocellulosic structure simulated by a thermogravimetry. Energy 35 (6), 2580–2586. https://doi.org/10.1016/j.energy.2010.02.054.

Essabir, H., Raji, M., Laaziz, S.A., Rodrique, D., Bouhfid, R., Qaiss, A.e.K., 2018. Thermo-mechanical performances of polypropylene biocomposites based on untreated, treated and compatibilized spent coffee grounds. Compos. B Eng. 149, 1–11.

Gallagher, L.W., McDonald, A.G., 2013. The effect of micron sized wood fibers in wood plastic composites. Maderas: Ciencia y Tecnologia 15 (3), 357–374. https://doi.org/10.4067/S0718-221X2013005000028.

García-García, D., Carbonell, A., Samper, M.D., García-Sanoguera, D., Balart, R., 2015. Green composites based on polypropylene matrix and hydrophobized spend coffee ground (SCG) powder. Compos. B Eng. 78, 256–265. https://doi.org/10.1016/j.compositesb.2015.03.080.

Goh, B.H.H., Ong, H.C., Chong, C.T., Chen, W.-H., Leong, K.Y., Tan, S.X., Lee, X.J., 2020. Ultrasonic assisted oil extraction and biodiesel synthesis of Spent Coffee Ground. Fuel 261, 116121.

Gurunathan, T., Mohanty, S., Nayak, S.K., 2015. A review of the recent developments in biocomposites based on natural fibres and their application perspectives. Compos. A Appl. Sci. Manuf. 77, 1–25. https://doi.org/10.1016/j.compositesa.2015.06.007.

Joshi, M., Brahma, S., Roy, A., Wazed Ali, S., 2017. Nano-calcium carbonate reinforced polypropylene and propylene-ethylene copolymer nanocomposites: Tensile vs. impact behavior. Fibers Polym. 18 (11), 2161–2169. https://doi.org/10.1007/s12221-017-7276-7.

Jung, K.W., Choi, B.H., Hwang, M.J., Jeong, T.U., Ahn, K.H., 2016. Fabrication of granular activated carbons derived from spent coffee grounds by entrapment in calcium alginate beads for adsorption of acid orange 7 and methylene blue. Bioresour. Technol. 219, 185–195. https://doi.org/10.1016/j.biortech.2016.07.098.

Kang, S.B., Oh, H.Y., Kim, J.J., Choi, K.S., 2017. Characteristics of spent coffee ground as a fuel and combustion test in a small boiler (6.5 kW). Renewable Energy 113, 1208–1214. https://doi.org/10.1016/j.renene.2017.06.092.

Karimah, A., Ridho, M.R., Munawar, S.S., Adi, D.S., Ismadi, Damayanti, R., Subiyanto, B., Fatriasari, W., Fudholi, A., 2021. A review on natural fibers for development of eco-friendly bio-composite: characteristics, and utilizations. J. Mater. Res. Technol. 13, 2442–2458.

Khan, M.Z.R., Srivastava, S.K., Gupta, M.K., 2020. A state-of-the-art review on particulate wood polymer composites: Processing, properties and applications. Polym. Test. 89 (May), 106721 https://doi.org/10.1016/j.polymertesting.2020.106721.

Kim, N.K., Lin, R.J.T., Bhattacharyya, D., 2014. Extruded short wool fibre composites: Mechanical and fire retardant properties. Compos. B Eng. 67, 472–480. https://doi.org/10.1016/j.compositesb.2014.08.002.

Lachheb, A., Allouhi, A., El Marhoune, M., Saadani, R., Kousksou, T., Jamil, A., Rahmoune, M., Oussouaddi, O., 2019. Thermal insulation improvement in construction materials by adding spent coffee grounds: An experimental and

simulation study. J. Cleaner Prod. 209, 1411–1419. https://doi.org/10.1016/j.jclepro.2018.11.140.
Martins, C.I., Gil, V., 2020. Processing–Structure–Properties of Cork Polymer Composites. Front. Mater. 7 (September), 1–12. https://doi.org/10.3389/fmats.2020.00297.
Martins, C.I., Gil, V., Rocha, S., 2022. Thermal, Mechanical, Morphological and Aesthetical Properties of Rotational Molding PE/Pine Wood Sawdust Composites. Polymers 14 (1), 193. https://doi.org/10.3390/polym14010193.
Massaro Sousa, L., Ferreira, M.C., 2019. Densification behavior of dry spent coffee ground powders: Experimental analysis and predictive methods. Powder Technol. 357, 149–157. https://doi.org/10.1016/j.powtec.2019.08.069.
Mata, T.M., Martins, A.A., Caetano, N.S., 2018. Bio-refinery approach for spent coffee grounds valorization. Bioresour. Technol. 247, 1077–1084.
McNutt, J., & He, Q. (Sophia). (2019). Spent coffee grounds: A review on current utilization. Journal of Industrial and Engineering Chemistry, 71, 78–88. https://doi.org/10.1016/j.jiec.2018.11.054.
Murayama, K., Ueno, T., Kobori, H., Kojima, Y., Suzuki, S., Aoki, K., Ito, H., Ogoe, S., Okamoto, M., 2019. Mechanical properties of wood/plastic composites formed using wood flour produced by wet ball-milling under various milling times and drying methods. Journal of Wood Science 65 (1). https://doi.org/10.1186/s10086-019-1788-2.
Mussatto, S.I., Machado, E.M.S., Carneiro, L.M., Teixeira, J.A., 2012. Sugars metabolism and ethanol production by different yeast strains from coffee industry wastes hydrolysates. Appl. Energy 92, 763–768. https://doi.org/10.1016/j.apenergy.2011.08.020.
Pickering, K.L., Efendy, M.G.A., Le, T.M., 2016. A review of recent developments in natural fibre composites and their mechanical performance. Compos. A Appl. Sci. Manuf. 83, 98–112. https://doi.org/10.1016/j.compositesa.2015.08.038.
Rahman, M.R., Huque, M.M., Islam, M.N., Hasan, M., 2009. Mechanical properties of polypropylene composites reinforced with chemically treated abaca. Compos. A Appl. Sci. Manuf. 40 (4), 511–517. https://doi.org/10.1016/j.compositesa.2009.01.013.
Rana, A.K., Mandal, A., Bandyopadhyay, S., 2003. Short jute fiber reinforced polypropylene composites: effect of compatibiliser, impact modifier and fiber loading. Compos. Sci. Technol. 63 (6), 801–806.
Reis, K.C., Pereira, L., Melo, I.C.N.A., Marconcini, J.M., Trugilho, P.F., Tonoli, G.H.D., 2015. Particles of coffee wastes as reinforcement in polyhydroxybutyrate (PHB) based composites. Mater. Res. 18 (3), 546–552. https://doi.org/10.1590/1516-1439.318114.
Renner, K., Móczó, J., Suba, P., Pukánszky, B., 2010. Micromechanical deformations in PP/lignocellulosic filler composites: Effect of matrix properties. Compos. Sci. Technol. 70 (7), 1141–1147. https://doi.org/10.1016/j.compscitech.2010.02.029.
Ronga, D., Pane, C., Zaccardelli, M., Pecchioni, N., 2016. Use of Spent Coffee Ground Compost in Peat-Based Growing Media for the Production of Basil and Tomato Potting Plants. Commun. Soil Sci. Plant Anal. 47 (3), 356–368. https://doi.org/10.1080/00103624.2015.1122803.
Rosa, S.M.L., Santos, E.F., Ferreira, C.A., Nachtigalt, S.M.B., 2009. Studies on the properties of rice-husk-filled-PP composites - Effect of maleated pp. Mater. Res. 12 (3), 333–338. https://doi.org/10.1590/S1516-14392009000300014.
Sallih, N., Lescher, P., Bhattacharyya, D., 2014. Factorial study of material and process parameters on the mechanical properties of extruded kenaf fibre/polypropylene composite sheets. Compos. A Appl. Sci. Manuf. 61, 91–107. https://doi.org/10.1016/j.compositesa.2014.02.014.
Sanchez-Silva, L., López-González, D., Villaseñor, J., Sánchez, P., Valverde, J.L., 2012. Thermogravimetric-mass spectrometric analysis of lignocellulosic and marine biomass pyrolysis. Bioresour. Technol. 109, 163–172. https://doi.org/10.1016/j.biortech.2012.01.001.
Sanjay, M.R., Siengchin, S., Parameswaranpillai, J., Jawaid, M., Pruncu, C.I., Khan, A., 2019. A comprehensive review of techniques for natural fibers as reinforcement in composites: Preparation, processing and characterization. Carbohydr. Polym. 207 (November 2018), 108–121. https://doi.org/10.1016/j.carbpol.2018.11.083.
Sefain, M.Z., El-Kalyoubi, S.F., 1984. Thermogravimetric studies of different celluloses. Thermochim Acta 75 (1–2), 107–113. https://doi.org/10.1016/0040-6031(84)85010-8.
Shinoj, S., Visvanathan, R., Panigrahi, S., 2010. Towards industrial utilization of oil palm fibre: Physical and dielectric characterization of linear low density polyethylene composites and comparison with other fibre sources. Biosyst. Eng. 106 (4), 378–388. https://doi.org/10.1016/j.biosystemseng.2010.04.008.
Soleimani, M., Tabil, L., Panigrahi, S., Opoku, A., 2008. The effect of fiber pretreatment and compatibilizer on mechanical and physical properties of flax fiber-polypropylene composites. J. Polym. Environ. 16 (1), 74–82. https://doi.org/10.1007/s10924-008-0102-y.
Srubar, W.V., Pilla, S., Wright, Z.C., Ryan, C.A., Greene, J.P., Frank, C.W., Billington, S. L., 2012. Mechanisms and impact of fiber-matrix compatibilization techniques on the material characterization of PHBV/oak wood flour engineered biobased composites. Compos. Sci. Technol. 72 (6), 708–715. https://doi.org/10.1016/j.compscitech.2012.01.021.
Taib, M. N. A. M., & Julkapli, N. M. (2018). Dimensional stability of natural fiber-based and hybrid composites. In: Jawaid, M., Thariq, M. & Saba, N. (Eds.), Mechanical and Physical Testing of Biocomposites, Fibre-Reinforced Composites and Hybrid Composites, 1sr Ed., pp. 61–79.
Tangmankongworakoon, N., 2019. An approach to produce biochar from coffee residue for fuel and soil amendment purpose. International Journal of Recycling of Organic Waste in Agriculture 8 (s1), 37–44. https://doi.org/10.1007/s40093-019-0267-5.
Tasdemır, M., Biltekin, H., Caneba, G.T., 2009. Preparation and Characterization of LDPE and PP—Wood Fiber Composites. J. Appl. Polym. Sci. 112, 3095–3102. https://doi.org/10.1002/app.29650. 10.1002/app.29650.
Thomason, J.L., Rudeiros-Fernández, J.L., 2018. A review of the impact performance of natural fiber thermoplastic composites. Front. Mater. 5 (September), 1–18. https://doi.org/10.3389/fmats.2018.00060.
Väisänen, T., Haapala, A., Lappalainen, R., Tomppo, L., 2016. Utilization of agricultural and forest industry waste and residues in natural fiber-polymer composites: A review. Waste Manage. 54, 62–73. https://doi.org/10.1016/j.wasman.2016.04.037.
Väisänen, T., Das, O., Tomppo, L., 2017. A review on new bio-based constituents for natural fiber-polymer composites. J. Cleaner Prod. 149, 582–596. https://doi.org/10.1016/j.jclepro.2017.02.132.
Yang, H.S., Kim, H.J., Park, H.J., Lee, B.J., Hwang, T.S., 2006. Water absorption behavior and mechanical properties of lignocellulosic filler-polyolefin bio-composites. Compos. Struct. 72 (4), 429–437. https://doi.org/10.1016/j.compstruct.2005.01.013.
Zanjani, J.S.M., Poudeh, L.H., Ozunlu, B.G., Yagci, Y.E., Menceloglu, Y., Saner Okan, B., 2020. Development of waste tire-derived graphene reinforced polypropylene nanocomposites with controlled polymer grade, crystallization and mechanical characteristics via melt-mixing. Polym. Int. 69 (9), 771–779. https://doi.org/10.1002/pi.6012.
Zarrinbakhsh, N., Wang, T., Rodriguez-Uribe, A., Misra, M., Mohanty, A.K., 2016. Characterization of wastes and coproducts from the coffee industry for composite material production. BioResources 11 (3), 7637–7653. https://doi.org/10.15376/biores.11.3.7637-7653. https://doi.org/10.15376/biores.11.3.7637-7653.